The Spherical Harmonic Method: Corroboration with Monte Carlo and Experiment

C.-H. Chang, C.-K. Lin, W. Liang*, N. Goldsman, I. D. Mayergoyz, P. Oldiges*, J. Melngailis
Dept. of Electrical Engineering, University of Maryland, College Park, MD 20742
*Digital Equipment Corporation, Hudson, MA 01749

***Abstract*—We show that the Spherical Harmonic method gives results for the space-depedent energy distribution function that agree with analytical band Monte Carlo simulations on a nanometer length scale, but are calculated approximately 1000 times faster. We also substantiate the Spherical Harmonic method by showing it gives values for MOSFET substrate current that agree with experiment without the use of fitting parameters. We explain the agreement through the use of asymptotic analysis.**

I. Introduction

In this work we provide strong evidence that the Spherical Harmonic (SH) method of device simulation is very capable of modeling hot-electron phenomena. Specifically, we show the following results which have not previously been demonstrated:

(1) That the SH can also give the energy distribution function, and that it agrees with spherical band MC, but is approximately a thousand times faster.

(2) That the SH method accurately models impact-ionization and substrate current in MOSFET's, and for the case we studied, did not require the use of any fitting parameters.

To demonstrate agreement between SH and MC we show results for the calculated energy distribution function throughout a a 0.05μm base BJT. The results indicate that the SH and MC agree over the entire energy and space domains, including regions where the electric field varies by as much as 200kV/cm over a distance of 0.02μm. Our comparisons to experiments are based on a 0.33μm effective channel length MOSFET, where we obtain agreement with substrate current as well as source-drain current in subthreshold, linear and saturation regions.

We offer an explanation as to why the SH method gives results that agree with MC by asymptotically solving the equations resulting from the spherical harmonic expansion of the BTE. These solutions, as well as the requirement to satisfy specific boundary conditions in phase space, indicate that higher order SH terms decay on the nanometer length scale.

II. Spherical Harmonic Device Model and Numerical Solution

The SH device model contains the Poisson equation and the current-continuity equation for holes. We account for electron transport with the Boltzmann equation.

$$\nabla_{\mathbf{r}}^2\phi(\mathbf{r}) = \frac{q}{\epsilon_s}\left[\int f(\mathbf{k},\mathbf{r})d\mathbf{k} - p(\mathbf{r}) + D(\mathbf{r})\right] \quad (1)$$

$$\frac{\nabla_{\mathbf{k}}}{\hbar}\varepsilon\cdot\nabla_{\mathbf{r}}f(\mathbf{k},\mathbf{r}) + \frac{e}{\hbar}\nabla_{\mathbf{r}}\phi(\mathbf{r})\cdot\nabla_{\mathbf{k}}f(\mathbf{k},\mathbf{r}) = \left[\frac{\partial f(\mathbf{k},\mathbf{r})}{\partial t}\right]_c \quad (2)$$

$$\nabla_{\mathbf{r}}\cdot[\mu_p p(\mathbf{r})\nabla_{\mathbf{r}}\phi(\mathbf{r}) + \mu_p V_t\nabla_{\mathbf{r}}p(\mathbf{r})] = R(\phi,n,p) \quad (3)$$

$f(\mathbf{k},\mathbf{r})$ is the distribution function; $p(\mathbf{r})$ is the hole concentration; $\phi(\mathbf{r})$ is the potential; $D(\mathbf{r})$ is the net doping concentration; $R(\phi,n,p)$ is the recombination rate; $V_t = K_BT/e$; ϵ_s is the dielectric constant of silicon;μ_p is the hole mobility; $\hbar$ is the Plank's constant. For collisions, we explicitly evaluate the collision integral using Fermi's Golden Rule and deformation potential theory [1], [2].

Now, we express the distribution function in terms of the following SH expansion:

$$f(\vec{r},\vec{k}) = \sum_{l=0}^{\infty}\sum_{m=-l}^{l} f_l^m(\vec{r},\varepsilon)Y_l^m(\theta,\psi) \quad (4)$$

Here $Y_l^m(\theta,\psi)$ are the spherical harmonic basis functions, θ and ψ are the polar and azimuthal angles of the wave-vector, respectively. $f_l^m(\vec{r},\varepsilon)$ represents the expansion coefficients. The eventual goal is to determine the coefficients and thereby the distribution function for the device. We showed previously that by substituting the spherical harmonics expansion for the distribution function into the BTE, while taking advantage of the recurrence and orthogonality relationships between spherical harmonics, the BTE can be transformed into an infinite set of identical expressions for the coefficients [1], [2].

$$\sum_{i=1}^{2}\left\{v(\varepsilon)\left[\frac{\partial}{\partial x_i} - qE_i(\vec{r})\left(\frac{\partial}{\partial\varepsilon} - \frac{l-1}{2}\frac{\gamma'(\varepsilon)}{\gamma(\varepsilon)}\right)\right]\hat{a}_i^- + v(\varepsilon)\left[\frac{\partial}{\partial x_i} - qE_i(\vec{r})\left(\frac{\partial}{\partial\varepsilon} + \frac{l+2}{2}\frac{\gamma'(\varepsilon)}{\gamma(\varepsilon)}\right)\right]\hat{a}_i^+\right\} f_l^m = \left[\frac{\partial f_l^m(\mathbf{k},\mathbf{r})}{\partial t}\right]_c \quad (5)$$

where $v(\varepsilon) = \sqrt{2m\gamma(\varepsilon)}/m\gamma'(\varepsilon)$, $\gamma'(\varepsilon) = d\gamma(\varepsilon)/d\varepsilon$, $\gamma(\varepsilon)$ represents the dispersion relation, and $E_i(\vec{r})$ is the electric field in the i direction. The sum over i represents the Cartesian directions of a 2-D device cross-section in real-space. The raising and lowering operators $\hat{a}_i^{\pm}$ which we developed to relate the coefficients are[1]:

0-7803-3775-1/97/$10.00 © 1997 IEEE.

$$\hat{a}_1^- f_l^m \equiv \frac{1}{2}\left\{-\alpha_{l-1}^m \alpha_l^m f_{l-1}^{m-1} + \alpha_{l-1}^{-m}\alpha_l^{-m} f_{l-1}^{m+1}\right\}$$
$$\hat{a}_1^+ f_l^m \equiv \frac{1}{2}\left\{\alpha_{l+1}^{-m+1}\alpha_l^{-m+1} f_{l+1}^{m-1} - \alpha_{l+1}^{m+1}\alpha_l^{m+1} f_{l+1}^{m+1}\right\}$$
$$\hat{a}_2^- f_l^m \equiv \alpha_{l-1}^{-m+1}\alpha_l^m f_{l-1}^m; \quad \hat{a}_2^+ f_l^m \equiv \alpha_{l+1}^m \alpha_l^{-m+1} f_{l+1}^m$$
$$\alpha_l^m = \sqrt{\frac{l+m}{2l+1}} \tag{6}$$

While a system of equations has been obtained to arbitrarily high order, we must truncate the system to actually obtain a solution. Since the scattering rate in silicon is relatively high, and silicon is a covalent semiconductor, a relatively low order truncation should be applicable. (This truncation will be verified later in the paper.) We therefore use an expansion which includes the first four spherical harmonics $(Y_0^0, Y_1^{-1}, Y_1^0, Y_1^0)$. After truncating, the total energy H is used as the independent energy variable as opposed to the kinetic energy ε, $(H = \varepsilon - q\phi)$[3]. We can then arrive at the following tractable expression for the symmetrical part of the distribution function throughout the device[1], [2]:

$$\begin{aligned}
&-\nabla\cdot\left[\frac{\gamma^{3/2}\tau}{\gamma'}\nabla F_0^0(\mathbf{r},H)\right] \\
&= \frac{3(\varrho-1)D_n^2 m^{*5/2}}{2\sqrt{2}\pi\hbar^3\rho\omega_n}\left(\frac{\gamma^{1/2}\gamma'}{e^{\hbar\omega_n/K_0T}-1}\right)\left\{\sqrt{\gamma^-}\gamma'^- \right. \\
&\times\left[F_0^0(\mathbf{r},H-\hbar\omega_n) - e^{\hbar\omega_n/K_0T}F_0^0(\mathbf{r},H)\right] \\
&\left.+\sqrt{\gamma^+}\gamma'^+\left[e^{\hbar\omega_n/K_0T}F_0^0(\mathbf{r},H+\hbar\omega_n) - F_0^0(\mathbf{r},H)\right]\right\} \\
&+\frac{3}{2}m^*\gamma^{1/2}\gamma'\left[\frac{2F_0^0(\mathbf{r},2H+\Delta_{ii}+q\phi)}{\tau_{0,ii}^{in}(2H+2q\phi+\Delta_{ii})} - \frac{F_0^0(\mathbf{r},H)}{\tau_{0,ii}^{out}(H+q\phi)}\right. \\
&+\frac{f_T}{\tau_{0,rec}^{out}(H+q\phi)}\exp\left(\frac{H-H_t}{K_BT_0}\right) \\
&\left.-\frac{1-f_T}{\tau_{0,rec}^{out}(H+q\phi)}F_0^0(\mathbf{r},H)\right]
\end{aligned} \tag{7}$$

where $1/\tau$ is the total scattering rate and $\gamma^{\pm} = \gamma(\mathbf{r}, H \pm \hbar\omega_n)$. The terms on the RHS of (7) reflect intervalley phonon scattering, impact ionization and SHR recombination.

To solve the system, we first discretize the BTE using new exponential fitting methods that are calibrated to the density of energy states in silicon. After discretization, we solve the model iteratively with various approaches including of the conjugate gradient method.

III. Results

A. MOSFET Simulation: Experimental Verification

We used the above model to simulate a 0.35μm effective channel length MOSFET. Values for the transport parameters used in these calculations are given in Table 1. It is worth noting that, where applicable, the transport parameter values we used are the same, or very similar to, the values employed in MOSFET Monte Carlo simulations[5]. For the case of surface scattering, it was not applicable to take values from [5] since we employed different transport models. Since these values are not well known, we chose those that gave the best fit to the experimental I-V characteristics.

Parameter	Value	Unit
D_{ac}	4.0	eV
D_{op}	7e8	eV/cm
$\hbar\omega_{op}$	0.05	eV
D_{ss}	5e14	V/eV
D_{is}	1.45e15	$1/cm^3$
UB_{ac}	2e7	cm/sec
UC_{ac}	7.5e6	$(V/cm)^{-2/3}(Kcm/sec)$
A_{ii}	1	

We found that the values we chose are reasonable when compared to those put forth by others[6], [7]. In Figs. 1 and 2 we show compare our calculated results I-V characteristics with the device. From the figures it is clear that agreement is obtained in the subthreshold, as well as linear and saturations regions of operation.

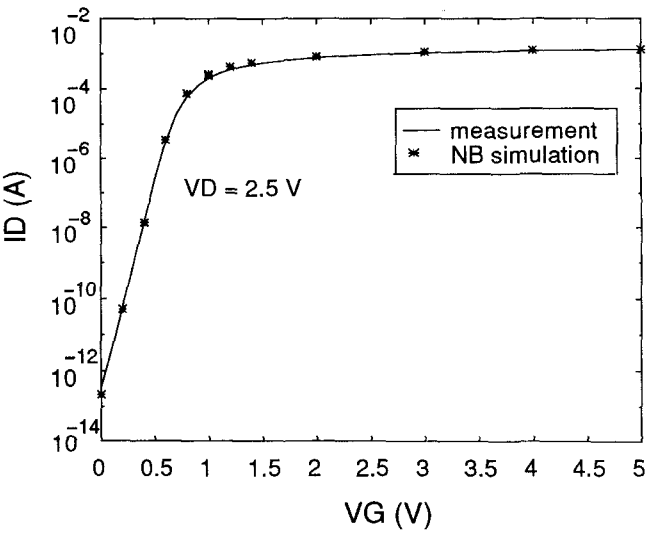

Fig. 1. Subthreshold MOSFET Current: The solid lines were measured while the asterisks were calculated by the SH approach

Next, we calculated substrate current by solving the current continuity equation for holes, and determining the hole current exiting the substrate contact. The hole generation rate due to impact ionization was obtained by equating it with the electron generation rate. The important aspect of this was that we determined the impact ionization rate directly from the impact ionization term in the BTE's collision integral. We used a random K model which accounts for the density as provided by the psuedopotential method of calculating band structures[4].

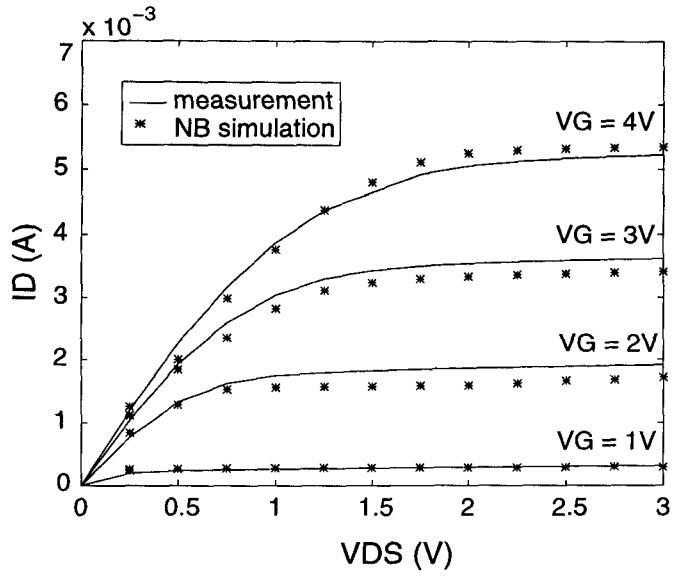

Fig. 2. Linear and Saturation MOSFET Current: The solid lines were measured while the asterisks were calculated by the SH approach

This model had previously been shown to agree with values for the impact ionization parameter α_{ii} which was developed for homogeneous electric fields. However, the model had not been tested for nonhomogeneous fields, especially not for an environment as complex as a MOSFET. We found that without any calibration, we calculated values for substrate current that were in agreement experiment. This agreement is shown in Fig. 3.

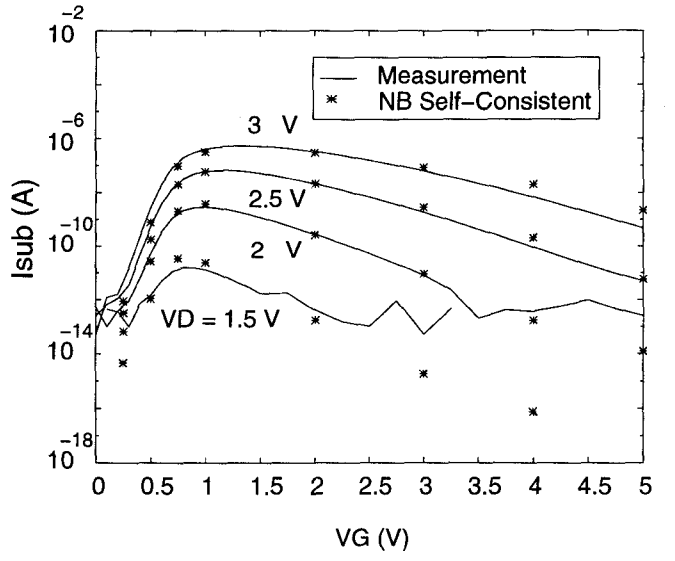

Fig. 3. MOSFET Substrate Current: The solid lines were measured while the asterisks were calculated by the SH approach

B. BJT Simulation: Monte Carlo Verification

We demonstrate that the SH approach gives results for the energy distribution function that agree with Monte Carlo simulations. To show this, we used the above formulation to simulate a $0.05\mu m$ base BJT. We chose the BJT because it represented a very aggressive challenge, with electric fields pointing in both directions, a narrow base of $50nm$, with fields varying as rapidly as 200kV/cm over distances as small as $20nm$. As a benchmark, we also simulated the same device using the Monte Carlo approach. The input parameters (analytical band structure, intervalley, optical and acoustic phonon scattering) were identical for both the SH and MC calculations. Since the main objective was to determine if the low-order SH method could respond to the rapid field variations of the BJTs, we performed both the Monte Carlo and the Spherical Harmonic calculations as post-processor simulations.

We show some example results below. In Fig. 4 we show the doping profile and resulting electric field with an applied potential of $V_{BE} = 1.0V$ and $V_{CB} = 3.0V$.

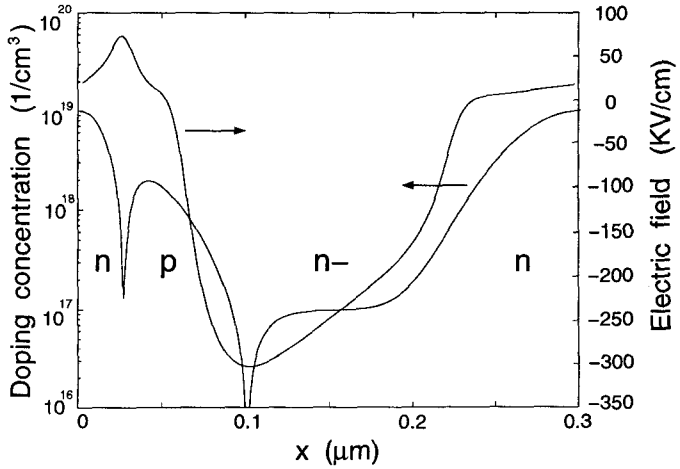

Fig. 4. Doping profile and electric field of BJT used in comparison simulations.

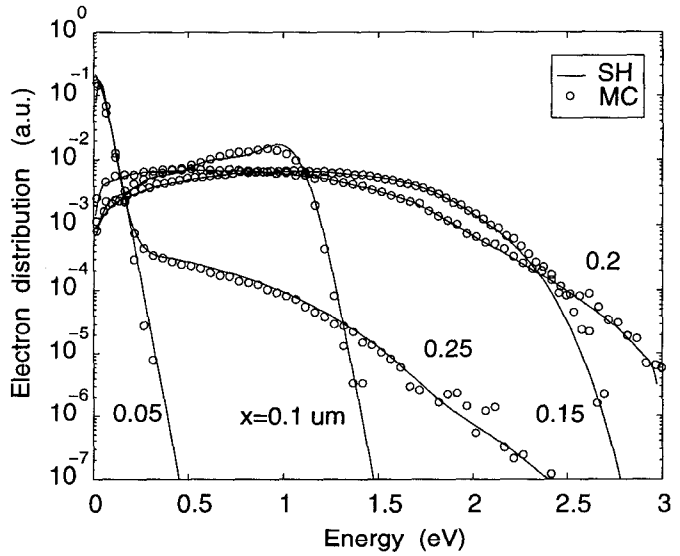

Fig. 5. Details of the energy distribution function calculated by SH (solid lines) and MC (open circles). Agreement between the approaches is very good.

In Fig. 5 we compare the details of the energy distribution function calculated by both the SH and MC approaches. In the plots, we compare the SH results (solid lines) with the MC results (open circles) at regular intervals along the device. Clearly, the SH and MC results are in very good agreement for the entire distribution function. We find this to be an extremely encouraging result, considering that the SH method required only $10sec$ to evaluate, while the MC approach took more than $10hours$ on a DEC Alpha 266MHz workstation. The large difference in CPU time is attributable to the deterministic nature of the SH approach, while the MC method requires considerable time to accumulate reasonable statistics for the high energy tail and to surmount the large potential barrier at the emitter-base junction. (The MC could probably be optimized but our attempts at statistical enhancement proved unreliable when subjected to scrutiny.)

IV. Analysis of Truncation and Discussion

We explain the agreement between SH and MC by asymptotic analysis. First of all, for very large values of SH index l, $l+1 \approx l$, and $F_{l+1} \approx F_l$. Under these conditions, equations (5) reduce to the following relatively simple expression.

$$v(H+q\phi)\frac{\partial F_n(x,H)}{\partial x} = -\frac{F_l(x,H)}{\lambda(H+q\phi)} \qquad (8)$$

where $\lambda(H+q\phi) = v(H+q\phi)\tau(H+q\phi)$ is a mean free path, the value of which depends on energy. For large energy λ becomes approximately constant, while for lower energies λ can be approximated as the following piecewise linear expression: $\lambda(H+q\phi) = \alpha \cdot (H+q\phi) + \beta$ within $[x_0,x]$ for a constant H. By integrating (8) over position space from x_0 to x for a constant H, using the chain rule $dx = \frac{dx}{d\varepsilon}d\varepsilon$, as well as approximating $E(x)$ as constant in the small interval, we can obtain

$$F_l(x,H) = F_l(x_0,H)\left[\left(\frac{\lambda(H+q\phi)}{\lambda(H+q\phi_0)}\right)^{\frac{1}{\alpha q E(x)}}\right] \qquad (9)$$

which simplifies to the following expression in the high energy region where λ is constant.

$$F_l(x,H) = F_l(x_0,H)\ exp\left(-\frac{x-x_0}{\lambda}\right) \qquad (10)$$

In high energy, (10) shows that F_l will decay exponentially in x-space with a characteristic length of λ. Depending on the transport model one is using, λ ranges from approximately $2nm$ to $5nm$ for energies greater than 1.5eV in silicon. This indicates that high-energy spherical harmonics decay very quickly in comparison with typical dimensions in deep submicron devices. For regions of low energy and low electric field, (9) ensures that F_l also decays very rapidly with distance. (While this is not immediately obvious, it is due to the relationship between ϕ and E, and the fact that λ is monotonically decreasing, ensures the exponent in (9) becomes very large, and the term in the square brackets is always less than unity.) For low to moderate energies, where there is a transition from a low electric field to a high one, or visa-versa, the monotonic nature of λ again insures that the square bracketed term in (9) will be small.

In addition to the asymptotic analysis for l, physical boundary conditions also suppress the magnitude of high order terms. For example, the physical requirement that the distribution function be single valued at the energy $\varepsilon = 0$ (is not dependent on angle at zero energy), leads to the requirement that all SH components with $l > 0$ must vanish at zero energy. Furthermore, the requirement that the distribution function is close to Maxwellian at the device contacts implies that higher order SH terms are negligible at these boundaries. Also, since in silicon the scattering rate is fairly high, and since it is a covalent semiconductor, we usually take the major scattering rates to be isotropic. This leads to scattering which tends to give rise to a distribution function which is largely spherical in nature. Finally, is one examines the generalized SH system given by equations (5), it is clear that the equations are only couple to nearest neighbors in l. It is therefore difficult to propagate information from low order terms to higher order ones, thereby minimizing the relative importance of higher order SH coefficients.

V. Acknowledgment

We are grateful to the National Science Foundation, the Semiconductor Research Corporation and the Microelectronics Research Laboratory for partially supporting this effort.

References

[1] K. A. Hennacy, Y.-J. Wu, N. Goldsman, and I. D. Mayergoyz, "Deterministic MOSFET Simulation Using a Generalized Spherical Harmonic Expansion of the Boltzmann Equation," *Solid-State Electronics*, vol. 38, pp. 1498–1495, 1995.

[2] W. Liang, N. Goldsman, I. Mayergoyz, and P. Oldiges, "2-dMOSFET modeling including surface effects and impact ionization by self-consistent solution of the Boltzmann, Poisson and hole-continuity equations," *IEEE Transactions on Elec. Dev.*, vol. 44, pp. 257–276, 1997.

[3] A. Gnudi, D. Ventura, and G. Baccarani, "Modeling Imapct Ionization in a BJT by Means of Spherical Harmonics Expansion of the Boltzmann Transport Equation," *IEEE Transactions on CAD*, vol. 12, p. 1706, 1993.

[4] Y.-J. Wu and N. Goldsman, "Deterministic Modeling of Impact Ionization with a Random-k Approximation and the Solution of the Multi-Band Boltzmann Transport Equation," *Journal of Applied Physics*, vol. 78, no. 8, 1995.

[5] C. Fiegna and E. Sangiorgi, "Modeling of High-Energy Electrons in MOS Devices at the Microscopic Level," *IEEE Trans. on Electron Devices*, vol. 40, no. 3, pp. 619–627, 1993.

[6] C. Sah, T. Ning, and L. Tschopp, "The scattering of electrons by surface charges and by lattice vibrations at the silicon-silicon dioxide interface," *Surface Science*, vol. 32, pp. 561–575, 1972.

[7] S. Goodnick, R. Gann, D. Ferry, and C. Wilmsen, "Surface roughness induced scattering and band tailing," *Surface Science*, vol. 113, pp. 233–238, 1982.